Mechanism of Phosphorescence Appropriate for the Long-Lasting Phosphors Eu^{2+}-Doped $SrAl_2O_4$ with Codopants Dy^{3+} and B^{3+}

F. Clabau,[†] X. Rocquefelte,[†] S. Jobic,*[,†] P. Deniard,[†] M.-H. Whangbo,*[,‡] A. Garcia,[§] and T. Le Mercier[||]

Laboratoire de Chimie des Solides, Institut des Matériaux Jean Rouxel, UMR 6502, 2 rue de la Houssinière, 44340 Nantes, France, Department of Chemistry, North Carolina State University, Raleigh, North Carolina 27695-8204, Institut de Chimie de la Matière Condensée de Bordeaux, CNRS, 87 avenue du Dr. A. Schweitzer, 33608 Pessac Cedex, France, and Rhodia, Centre de Recherches d'Aubervilliers, 52 rue de la Haie-Coq, 93308 Aubervilliers Cedex, France

Received April 11, 2005. Revised Manuscript Received June 8, 2005

The existing mechanisms proposed to explain the phosphorescence of $SrAl_2O_4$:Eu^{2+},Dy^{3+} and related phosphors were found to be inconsistent with a number of important experimental and theoretical observations. We formulated a new mechanism of phosphorescence on the basis of the facts that the d orbitals of Eu^{2+} are located near the conduction band bottom of $SrAl_2O_4$, that the Eu^{2+} concentration decreases during UV excitation, and that trace amounts of Eu^{3+} are always present in these phosphors. In our mechanism, some Eu^{2+} ions are oxidized to Eu^{3+} under UV, and the released electrons are trapped at the oxygen vacancy levels located in the vicinity of the photogenerated Eu^{3+} cations. The phosphorescence arises from the recombination of these trapped electrons around the photogenerated Eu^{3+} sites with emission at 520 nm. The codopant Dy^{3+} enhances the phosphorescence by increasing the number and the depth of electron traps, and the codopant B^{3+} enhances the phosphorescence by increasing the depth of electron traps. We also probed the origin of another emission at 450 nm of $SrAl_2O_4$:Eu^{2+} that occurs at low temperatures. Our analysis indicates that this emission is caused by a charge transfer from oxygen to Eu^{3+} cations and is associated with a hole trapping.

1. Introduction

Phosphorescence (or afterglow) refers to the light emission of an insulator that persists at room temperature after stopping excitation (usually UV irradiation).[1−3] This delayed light emission arises from the fact that charge carriers (i.e., electrons and/or holes) generated by the excitation are trapped at certain defect sites, and their detrapping is thermally activated. The term "phosphorescence" may also refer to a radiative fluorescence-type de-excitation delayed by more than 10^{-8} s, due commonly to the spin-forbidden nature of de-excitation (e.g., the $^2E \rightarrow {}^4A_2$ emission for Cr^{3+}). In our work the term "phosphorescence" refers exclusively to the phenomenon of an afterglow with emission lasting several minutes to several hours.

Besides luminescent centers, the phosphorescence phenomenon requires the presence of certain discrete levels within the forbidden band gap, which are associated with chemical and/or physical defects of the host lattice (e.g., dopants and vacancies). Under UV irradiation, some electrons and/or holes generated by the excitation are trapped in such localized levels. Due to a spatial separation between these defects and the luminescent centers (or more precisely, due to the lack of their orbital overlap), the probability of direct recombination is very low. Consequently, trapped charge carriers are maintained in a metastable state (i.e., the excitation energy is stored), as long as there is no energy supply for detrapping them and hence inducing their recombination. Two factors affect the energy needed for detrapping. The major one is the trap depth E_T, which refers generally to the energy difference between the trap level and the valence band (VB) top for a hole trap, and that between the conduction band (CB) bottom and the trap level for an electron trap. The other factor, often neglected, is the strength of interaction between the trapped charge carrier and the lattice. While use of thermal annealing or a laser light is necessary to detrap for scintillators, the thermal energy available at ambient temperature is enough for phosphorescent materials.

The lifetime τ of a trapped charge carrier is inversely proportional to the detrapping probability, and depends exponentially on the ratio of the trap depth to the thermal energy, E_T/k_BT. Consequently, the lifetime τ, and thus luminescence, is longer when the detrapping requires a higher energy. However, the observation of luminescence by naked eye requires a sufficient luminous flux, i.e., a sufficiently fast detrapping process. In industry, the phosphorescence decay time is defined as the duration from the moment of stopping the light excitation to the moment when the emission light intensity is reduced to 0.32 mCd/m^2 (i.e.,

[†] Institut des Matériaux Jean Rouxel.
[‡] North Carolina State University.
[§] Institut de Chimie de la Matière Condensée de Bordeaux.
[||] Centre de Recherches d'Aubervilliers.

(1) Blasse, G.; Grabmaier, B. C. *Luminescence materials*; Springer-Verlag: Berlin, 1994.
(2) McKeever, S. *Thermoluminescence of solids*; Cambridge Press University, Cambridge, 1988.
(3) Shionoya, S.; Yen, W. *Phosphor handbook*; CRC Press: New York, 1999.

10.1021/cm050763r CCC: $30.25
Published on Web 07/01/2005

100 times the perception limit of the human eye). The detrapping energy of $SrAl_2O_4:Eu^{2+},Dy^{3+},B^{3+}$ is 0.65 eV,[4] which appears to be the energy depth leading to an outstanding phosphorescent material.

Until a few years ago, the only practical phosphorescent compound was zinc sulfide codoped with copper and cobalt, $ZnS:Cu^{+},Co^{2+}$.[5] Due to several drawbacks of this compound, applications of phosphorescence had been limited. First, the intrinsic decay time is short (1 h), so its applications (i.e., watches, clocks, painting, etc.) require the addition of radioisotopes such as ^{3}H and ^{147}Pm. Second, the emission intensity is low, so a large amount of the compound should be incorporated into the host (up to 30% in weight for painting), hence degrading the physical and mechanical properties of the host. Third, the compound degrades in the presence of moisture, which requires an encapsulation for its outdoor use.

In 1995, Murayama et al. reported that $SrAl_2O_4:Eu^{2+},Dy^{3+},B^{3+}$ has greatly enhanced phosphorescence properties compared not only with $SrAl_2O_4:Eu^{2+}$ but also with $ZnS:Cu^{+},Co^{2+}$.[6] In addition to a higher chemical stability, the intensity and the duration of the phosphorescence of $SrAl_2O_4:Eu^{2+},Dy^{3+},B^{3+}$ make it possible to envisage a continuous light emission during a whole night now (10 h), hence greatly renewing interests in the phosphorescence phenomenon. As summarized in Table 1, a large number of new compounds discovered since 1995 shows phosphorescence lasting longer than 1 h. These compounds have a wide range of emission colors (e.g., violet, blue, green, red, pink, orange, yellow). Potential applications of these new phosphors are numerous, especially in the areas of safety improvement and energy saving (e.g., traffic signs, emergency signs, safety clothes, advertising, etc.).

Matsuzawa et al.[4] proposed a phosphorescence mechanism for $SrAl_2O_4:Eu^{2+},Dy^{3+}$ which invokes a reduction of Eu^{2+} to Eu^{+} and then a trapping of holes by Dy^{3+}. Two alternative mechanisms, proposed by Aitasalo et al.[7] and by Beauger,[8] invoke also a hole trapping but with an energy transfer process. As will be discussed later, all these mechanisms are not consistent with a number of important experimental and theoretical facts. In the present work, we review these observations in some detail and propose a new phosphorescence mechanism for $SrAl_2O_4:Eu^{2+}$ and codoped systems $SrAl_2O_4:Eu^{2+},Dy^{3+}$ and $SrAl_2O_4:Eu^{2+},Dy^{3+},B^{3+}$.

Our work is organized as follows. The structural and luminescence properties of $SrAl_2O_4:Eu^{2+}$ and its codoped analogues are summarized in section 2. In section 3, we describe the three phosphorescence mechanisms proposed for codoped $SrAl_2O_4:Eu^{2+}$ and $CaAl_2O_4:Eu^{2+}$ and then discuss their shortcomings. In section 4 we propose a new phosphorescence mechanism for codoped $SrAl_2O_4:Eu^{2+}$ and $CaAl_2O_4:Eu^{2+}$ and subsequently show that it accounts for all important experimental and theoretical observations. Finally, essential findings of our work are summarized in section 5.

Table 1. Emission Colors of the Phosphors with Phosphorescence Lasting Longer than 1 h

(a) aluminates	$SrAl_2O_4:Eu^{2+},Dy^{3+},B^{3+}$ (green),[6] $CaAl_2O_4:Eu^{2+},Nd^{3+},B^{3+}$ (blue),[7] $BaAl_2O_4:Eu^{2+},Dy^{3+}$ (green),[41] $MgAl_2O_4:Ce^{3+}$ (green),[42] $CaAl_2O_4:Ce^{3+}$ (purple),[43] $CaAl_2O_4:(Ce^{3+},Tb^{3+})$ (green),[44] $CaAl_2O_4:(Ce^{3+},Mn^{2+})$ (green),[45] $BaAl_2O_4:Ce^{3+},Dy^{3+}$ (blue),[46] $MgAl_2O_4:Tb^{3+}$ (green),[47] $CaAl_2O_4:Tb^{3+}$ (green),[48] $Sr_4Al_{14}O_{25}:Eu^{2+},Dy^{3+},B^{3+}$ (blue),[49] $SrAl_4O_7:Eu^{2+},Dy^{3+}$ (blue),[50] $CaYAl_3O_7:Ce^{3+}$ (blue),[51] $Ca_{12}Al_{14}O_{33}:Eu^{2+},Nd^{3+}$ (indigo)[52]
(b) silicates	$M_3MgSi_2O_8:Eu^{2+},Dy^{3+}$ (blue),[53] $M_2MgSi_2O_7:Eu^{2+},Dy^{3+}$ (blue to green),[54] $CaMgSi_2O_6:Eu^{2+},Dy^{3+}$ (blue),[55] $Sr_2ZnSi_2O_7:Eu^{2+},Dy^{3+}$ (blue),[56] $MgSiO_3:(Eu^{2+},Mn^{2+}),Dy^{3+}$ (red),[57] $CdSiO_3:Mn^{2+}$ (orange),[58] $CdSiO_3:Sm^{3+}$ (pink)[59]
(c) aluminosilicates	$Ca_2Al_2SiO_7:Eu^{2+},Dy^{3+}$ (blue),[60] $Sr_2Al_2SiO_7:Eu^{2+},Dy^{3+}$ (green),[60] $Ca_2Al_2SiO_7:Ce^{3+}$ (purple),[61] $Ca_2Al_2SiO_7:(Ce^{3+},Mn^{2+})$ (yellow),[57] $CaAl_2Si_2O_8:Eu^{2+},Dy^{3+}$ (blue)[62]
(d) other oxides	$(Zn,Mg)Ga_2O_4:Mn^{2+}$ (green),[63] $MO:Eu^{3+}$ (orange to red),[64] $SrO:Pb^{2+}$ (purple),[65] $Y_2O_3:Eu^{3+},Mg^{2+},Ti^{4+}$ (red),[66] $Zn_3(PO_4)_2:Mn^{2+},Ga^{3+}$ (red),[67] $MgGeO_3:Mn^{2+},Yb^{3+}$ (red)[68]
(e) oxysulfides	$Y_2O_2S:Eu^{3+},Mg^{2+},Ti^{4+}$ (orange to red),[69] $Y_2O_2S:Sm^{3+}$ (orange/red),[70] $Y_2O_2S:Tm^{3+}$ (yellow/orange)[71]
(f) sulfides	$ZnS:Cu^{+},Co^{2+}$ (green),[5] $CaS:Eu^{2+},Tm^{3+}$ (red),[72] $CaS:Bi^{3+},Tm^{3+}$ (blue),[73] $CaGa_2S_4:Eu^{2+},Ho^{3+}$ (yellow)[74]

2. Structural and Luminescence Properties of $SrAl_2O_4:Eu^{2+}$ and Its Codoped Analogues

2.1. Structural Characteristics. The aluminate $SrAl_2O_4$ exists in two crystallographic forms, and a reversible transition between the two occurs at 650 °C.[9] The structure of the low-temperature phase (monoclinic, space group $P2_1$, $a = 8.447$ Å, $b = 8.816$ Å, $c = 5.163$ Å, $\beta = 93.42°$) is well established,[10] but that of the high-temperature phase (hexagonal, space group $P6_322$, $a = 5.140$ Å, $c = 8.462$ Å) is not.[9] The structure of the low-temperature phase has a three-dimensional network of corner-sharing AlO_4 tetrahedra, which has channels in the a- and c-directions where the Sr^{2+} ions are located (Figure 1). There are two crystallographically different sites for Sr^{2+} (Wyckoff position 2a), which have identical coordination numbers (i.e., 6+1), similar average Sr−O distances (i.e., 2.695 Å and 2.667 Å) and similar individual Sr−O distances. The two environments differ only by a slight distortion of their "square planes". The Sr^{2+} and Eu^{2+} ions are very similar in their ionic size (i.e., 1.21 and 1.20 Å, respectively). Consequently, when occupied by Eu^{2+} ions, the two different Sr^{2+} sites will have a quite similar

(4) Matsuzawa, T.; Aoki, Y.; Takeuchi, N.; Maruyama, Y. *J. Electrochem. Soc.* **1996**, *143*, 2670.
(5) Hoogenstraaten, W.; Klasens, H. A. *J. Electrochem. Soc.* **1953**, *100*, 336.
(6) Murayama, Y.; Takeuchi, N.; Aoki, Y.; Matsuzawa, T. U.S. Patent No. 5,424,006, 1995.
(7) Aitasalo, T.; Deren, P.; Hölsa, J.; Jungner, H.; Krupa, J.; Lastusaari, M.; Legendziewicz, J.; Niittykoski, J.; Strek, W. *J. Solid State Chem.* **2003**, *171*, 114.
(8) Beauger, C. Thesis, Université de Nice, Nice, France, 1999.
(9) Ito, S.; Banno, S.; Inagaki, M. *Z. Physik. Chem.* **1977**, *105*, 173.
(10) Schulze, A.; Mueller-Buschbaum, H. *Z. Anorg. Allg. Chem.* **1981**, *475*, 205.

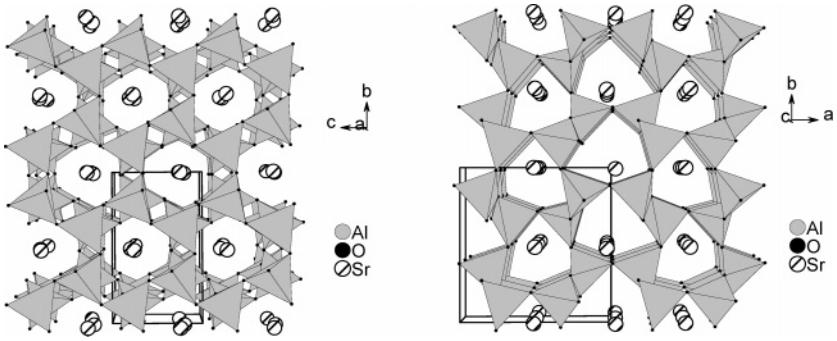

Figure 1. Schematic views of the monoclinic phase of $SrAl_2O_4$ along the a- and c-directions.

local distortion, so that the Eu^{2+} ions located at the two different Sr^{2+} sites will have very similar local environments.

The phosphorescence in the monoclinic phase of the phosphor $SrAl_2O_4$:Eu^{2+} has been observed when prepared in the form of a thin layer[11] or a crystal,[12,13] by solid-state reactions (at 1300 °C during few hours),[4] a sol−gel route (at 1150 °C),[14] a microwave route,[15] and a combustion method.[16] Europium is introduced in the reaction mixture in its oxidized state Eu^{3+} (Eu_2O_3), and phosphorescence appears only after a reducing treatment (in situ or afterwards).[8] Luminescence measurements show that after this reducing treatment, europium is mainly present in the reduced form Eu^{2+},[4] but Mössbauer measurements reveal that there remains roughly 5 to 10% of Eu^{3+} (hereafter referred to as residual Eu^{3+}).[17] XANES measurements show that the codopant dysprosium is present in its stable form Dy^{3+}.[18]

2.2. Dopant and Codopant Sites. The sites of the dopants and codopants of $SrAl_2O_4$ are dictated by their ionic radii. The Eu^{2+} (1.20 Å), Eu^{3+} (1.01 Å), and Dy^{3+} (0.97 Å) ions can readily occupy the Sr^{2+} (1.21 Å) ion sites,[19] as confirmed by EPR measurements.[20] The two crystallographically different Sr^{2+} sites are very similar, so it is expected that the luminescent ions Eu^{2+} are present at both sites. This expectation is corroborated by EPR measurements.[21] The fact that Sr^{2+} and Eu^{2+} ions have very close ionic radii explains why Eu^{3+} ions introduced in the Sr^{2+} sites of $SrAl_2O_4$ are easily reduced to Eu^{2+}.[8] The codopant B^{3+} ions (0.11 Å) are expected to occupy the Al^{3+} ion sites (0.39 Å), which is confirmed by IR and NMR measurements.[22] However, due to the large difference in the ionic radii, the substitution of B^{3+} for Al^{3+} will lead to a strong local strain, which should be partially released by forming trigonal planar units BO_3. The latter was observed by IR and NMR measurements.[23,24]

2.3. Probable Vacancies. The formation of the byproduct $Sr_3Al_2O_6$ during the synthesis of $SrAl_2O_4$ [8] as well as the thermoluminescence (TL) measurements carried out for the stoichiometric and nonstoichiometric samples of $SrAl_2O_4$:Eu^{2+} [25] indicate that $SrAl_2O_4$ tends to have strontium vacancies (V_{Sr}), and hence oxygen vacancies (V_O) due to the requirement of charge neutrality, leading to $Sr_{1-\delta}Al_2O_{4-\delta}$ ($\delta > 0$). This is consistent with the result of bond valence sum calculations,[26] which lead to charges of ~1.75 for Sr and ~3 for Al. Aluminum vacancies (V_{Al}) might exist as well, but would be energetically unfavorable to form because the Al−O bonds are short and strong. Due to the requirement of charge neutrality and the absence of oxygen in the synthesis atmosphere, the codoping with Dy^{3+} should enhance the cation deficiency.

2.4. Luminescence Characteristics. The luminescence properties of $SrAl_2O_4$:Eu^{2+} were discovered in 1968.[27,28] The emission spectrum at room temperature displays a broad band with a maximum at 520 nm, leading to the green luminescence of the materials under normal conditions.[4] As the temperature is decreased, an additional peak occurs in the emission spectrum at 450 nm.[29] When the Eu concentration is higher, the intensity of the 520 nm emission increases and that of the 450 nm emission decreases.[8] This suggests that an energy transfer occurs from the 450 nm emission to the 520 nm emission.[29]

Poort et al.[29] suggested that the 450 and 520 nm emission bands originate from the $4f^65d^1 \rightarrow 4f^7(^8S_{7/2})$ transition of Eu^{2+} located at the two different crystallographic strontium sites. The disappearance of the 450 nm emission when the temperature is increased[8] is consistent with the idea of energy transfer. However, the assignment of the Eu^{2+} $4f^65d^1 \rightarrow 4f^7(^8S_{7/2})$ transition to both emissions of $SrAl_2O_4$:Eu^{2+} is not supported for the following reasons:

(1) The two Sr sites are chemically nearly identical, so that the Eu^{2+} ions located at these two different Sr sites should emit in a similar energy range (and not with a

(11) Kato, K.; Tsutai, I.; Kamimura, T.; Kaneko, F.; Shinbo, K.; Ohta, M.; Kawakami, T. *J. Lumin.* **1999**, *82*, 213.
(12) Katsumata, T.; Nabae, T.; Sasajima, K.; Matsuzawa, T. *J. Cryst. Growth* **1998**, *183*, 361.
(13) Jia, W.; Yuan, H.; Lu, L.; Liu, H.; Yen, W. *J. Cryst. Growth* **1999**, 200, 179.
(14) Tang, Z.; Zhang, F.; Zhang, Z.; Huang, C.; Lin, Y. *J. Eur. Ceram. Soc.* **2000**, *20*, 2129.
(15) Geng, J.; Wu, Z. *J. Mater. Synth. Proc.* **2002**, *10*, 245.
(16) Peng, T.; Yang, H.; Pu, X.; Hu, B.; Jiang, Z.; Yan, C. *Mater. Lett.* **2004**, *58*, 352.
(17) Clabau, F. Thesis, Université de Nantes, Nantes, France, 2005 (restricted diffusion up to 2010).
(18) Rhodia Electronics and Catalysis. Private communication, 2001.
(19) Shannon, R. *Acta Crystallogr., A* **1976**, *32*, 751.
(20) Nakamura, T.; Kaiya, K.; Takahashi, T.; Matsuzawa, T.; Ohta, M., Rowlands, C.; Smith, G.; Riedi, P. *Phys. Chem. Chem. Phys.* **2001**, *3*, 1721.
(21) Kaiya, K.; Takahashi, N.; Nakamura, T.; Matsuzawa, T.; Smith, G.; Riedi, P. *J. Lumin.* **2000**, *87−89*, 1073.
(22) Nag, A.; Kutty, T. *J. Alloys Compd.* **2003**, *354*, 221.
(23) Rhodia Electronics and Catalysis. Private communication, 2001.
(24) Niittykoski, J.; Aitasalo, T.; Hölsa, J.; Jungner, H.; Lastusaari, M.; Parkkinen, M.; Tukia, M. *J. Alloys Compd.* **2004**, *374*, 108.
(25) Abbruscato, V. *J. Electrochem. Soc.* **1971**, *118*, 930.
(26) Breese, N.; O'Keeffe, M. *Acta Crystallogr. B* **1991**, *47*, 192.
(27) Palilla, F.; Levine, A.; Tomkus, M. *J. Electrochem. Soc.* **1968**, *115*, 642.
(28) Blasse, G.; Bril, A. *Philips Res. Rep.* **1968**, *23*, 201.
(29) Poort, S.; Blockpoel, W.; Blasse, G. *Chem. Mater.* **1995**, *7*, 1547.

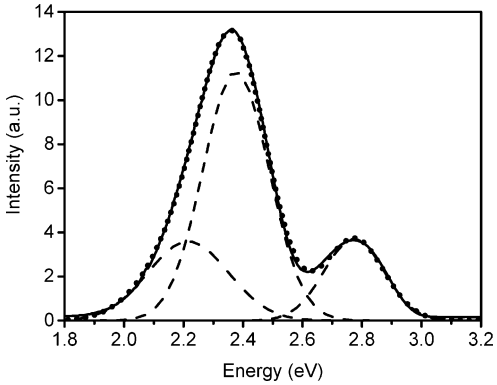

Figure 2. Deconvolution of the 520 and 450 nm fluorescence peaks of $Sr_{0.98}Al_2O_4:Eu^{2+}_{0.02}$, measured at the 310 nm excitation light at 100 K using a Fluorolog-3 spectrofluorometer.

0.37 eV difference). Formally, the 520 nm emission spectrum can be deconvoluted in terms of two Gaussian peaks centered at 515 nm and 545 nm (i.e., two peaks separated by 0.13 eV; Figure 2). Similarly, the deconvolution of the only emission peak of $BaAl_2O_4:Eu^{2+}$ at 4.2 K[29] shows two peaks at 510 and 540 nm. This suggests that the 520 nm emission originates from the Eu^{2+} $4f^65d^1 \rightarrow 4f^7(^8S_{7/2})$ transitions associated with the Eu^{2+} ions randomly distributed at the two different Sr^{2+} sites. There is no need to assign the 450 nm emission to Eu^{2+} $4f^65d^1 \rightarrow 4f^7$ $(^8S_{7/2})$ transitions.

(2) The low-temperature luminescence spectrum of $SrAl_2O_4$:Eu samples prepared in air (hence with almost only Eu^{3+} ions) shows only the peak at 450 nm.[8] The 520 nm emission appears only when the samples are annealed under a reducing atmosphere. It is highly unlikely that partial reduction of Eu^{3+} cations takes place only for those occupying one of the two Sr^{2+} sites. Therefore, it should be concluded that the green emission at 520 nm is due to the Eu^{2+} $4f^65d^1 \rightarrow 4f^7(^8S_{7/2})$ transition, while the blue emission at 450 nm results from another de-excitation mechanism.

(3) When the Y^{3+} concentration increases in $SrAl_2O_4$:Eu^{2+},Y^{3+}, the intensity of the 450 nm blue fluorescence decreases strongly, but that of the 520 nm green emission remains constant.[8] Likewise, when the Dy^{3+} concentration increases in $SrAl_2O_4:Eu^{2+},Dy^{3+}$, the intensity of the 450 nm blue emission intensity remains constant, but that of the 520 nm green emission decreases.[8] The different influences of the codopants Y^{3+} and Dy^{3+} on the two emission intensities show that the 450 and 520 nm emissions must be different in nature.

(4) The decay time of the 450 nm fluorescence emission,[30] which is observed only at low temperatures where no detrapping occurs, is much shorter than that of the 520 nm emission in $SrAl_2O_4:Eu^{2+}$ (0.7 vs 1.7 μs vs at 4.2 K). In contrast, the decay times of the two Eu^{2+} emissions in $BaAl_2O_4:Eu^{2+}$ (at 510 and 540 nm) are practically the same (1.5 μs vs 1.4 μs). This finding again suggests that the blue and green emissions are of different origin.

(5) $CaAl_2O_4$ has a monoclinic structure with three nonequivalent Ca sites, and Eu^{2+} ions occupy only one kind of the Ca sites due to the size matching requirement.[7] At room

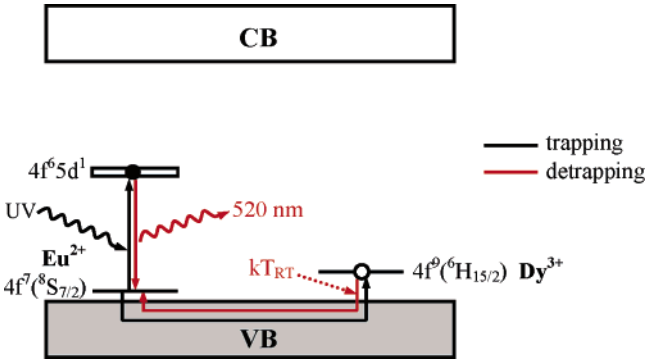

Figure 3. Phosphorescence mechanism proposed by Matsuzawa et al. for $SrAl_2O_4:Eu^{2+},Dy^{3+}$.

temperature, $CaAl_2O_4:Eu^{2+},Nd^{3+}$ samples exhibit a broad blue emission peaking at 440 nm assigned to the Eu^{2+} $4f^65d^1 \rightarrow 4f^7(^8S_{7/2})$ transition. At low temperatures, they show an unresolved emission peaking at ~450 nm,[31] which is similar in energy to the 450 nm emission of $SrAl_2O_4:Eu^{2+}$. The invariability in the position of the blue emission suggests again that its origin is not related to the Eu^{2+} cations.

3. Existing Mechanisms for the Phosphorescence of Codoped $SrAl_2O_4:Eu^{2+}$ and $CaAl_2O_4:Eu^{2+}$

So far, three different mechanisms have been proposed to explain the phosphorescence of codoped $SrAl_2O_4:Eu^{2+}$ and $CaAl_2O_4:Eu^{2+}$. In this section, we describe these mechanisms and discuss their shortcomings. It must be pointed out that the role of the codopant B^{3+} ions has remained unclear. [32]

3.1. Mechanism of Matsuzawa et al. The mechanism of Matsuzawa et al. proposed for $SrAl_2O_4:Eu,Dy$[4] (Figure 3) relies largely on the photoconductivity study of powder $SrAl_2O_4:Eu^{2+}$ samples,[25] which showed that UV irradiation induces a hole-type photoconductivity and hence suggested the existence of a hole trapping. The excitation and emission spectra was associated with Eu^{2+}, so that

$$Eu^{2+}\ (4f^7) + h\nu \rightarrow Eu^{2+}*\ (4f^65d^1)$$

$$Eu^{2+}*\ (4f^65d^1) \rightarrow Eu^{2+}\ (4f^7) + h\nu'$$

Matsuzawa et al. suggested that the holes originate from the capture of electrons from the VB by the $Eu^{2+}*$ ions, and the codopants Dy^{3+} trap these holes, i.e.,

$$Dy^{3+}\ (4f^9) + h^+ \rightarrow Dy^{4+}\ (4f^8)$$

and that the return of the trapped holes to the Eu sites for delayed emission is triggered by thermally activated electron promotion from the top of the VB top to Dy^{4+}. We note that trapping of holes by cationic vacancies was also considered by others.[7,33] In their mechanism, Matsuzawa et al. made two crucial assumptions: the fundamental level (i.e., the ground state) of the $4f^7$ configuration of Eu^{2+} is close in energy to the top of the valence band (i.e., 0.06 eV), and

(30) Poort, S.; Meijerink, A.; Blasse, G. *J. Phys. Chem. Solids* **1997**, *58*, 1451.
(31) Jia, W.; Yuan, H.; Lu, L.; Liu, H.; Yen, W. *J. Cryst. Growth* **1999**, *200*, 179.
(32) Nag, A.; Kutty, T. *Mater. Res. Bull.* **2004**, *39*, 331.
(33) Ohta, M.; Takami, M. *J. Electrochem. Soc.* **2004**, *151*, G171.

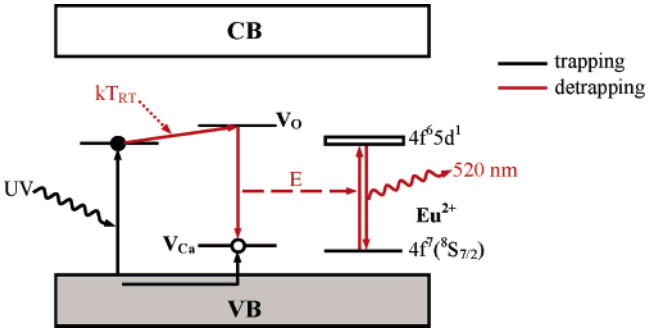

Figure 4. Phosphorescence mechanism proposed by Aitasalo et al. for $CaAl_2O_4:Eu^{2+},Nd^{3+}$.

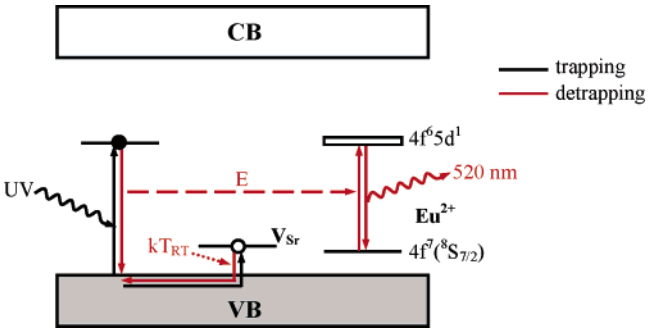

Figure 5. Phosphorescence mechanism proposed by Beauger for $SrAl_2O_4:Eu^{2+}$.

the Eu^{2+} ion excited by irradiation becomes an excited Eu^{+}* ion upon electron capture,

$$Eu^{2+}* (4f^6 5d^1) + e^- \rightarrow Eu^{+}* (4f^7 5d^1)$$

3.2. Mechanism of Aitasalo et al. The phosphorescence mechanism of Aitasalo et al. proposed for $CaAl_2O_4:Eu^{2+}$, Nd^{3+} (and easily extrapolated to the Sr derivatives)[7] (Figure 4) is based on the realization that the formation of the highly unstable species Eu^{+}* under UV or visible irradiation is highly unlikely. The reduction of Eu^{3+} into Eu^{2+} in oxides already requires a high energy (~3.7 eV), and the further reduction of Eu^{2+} should require a much higher energy.[1] To retain the hole trapping process suggested from the photoconductivity experiments, Aitasalo et al. assumed the occurrence of energy transfer to Eu^{2+} and proposed that the UV excitation promotes an electron from the VB to a discrete level of unknown origin, while the hole created in the VB is trapped by an alkaline earth vacancy level V_{Ca}. Then, Aitasalo et al. assumed that the thermal energy allows the transfer of the electron from the discrete level of unknown origin to an oxygen vacancy level V_O, from which a recombination takes place toward the V_{Ca} level. The energy released is then transferred to an Eu^{2+} ion, which is excited and then is de-excited instantaneously. In this mechanism, the role of Nd^{3+} codoping is considered to increase the number of cation vacancies.

3.3. Mechanism of Beauger. The mechanism of Beauger proposed for $SrAl_2O_4:Eu^{2+}$ [8] (Figure 5) is similar to that of Aitasalo et al. in invoking the electron excitation into a discrete level of unknown origin, the trapping of the holes created in the VB at cation vacancy levels and the occurrence of energy transfer to Eu^{2+}. However, he assumed that the thermal energy enables the detrapping of the holes to the valence band, and then their recombination with the electrons present in the aforementioned discrete levels of unknown origin. As for the role of the codopant Dy^{3+}, he assumed that UV radiation would initiate the heteronuclear intervalence charge transfer,

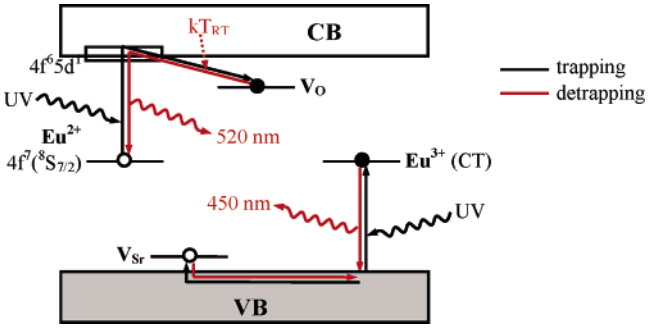

Figure 6. Phosphorescence mechanism proposed in the present work for $SrAl_2O_4:Eu^{2+},Dy^{3+},B^{3+}$.

$$Eu^{2+} + Dy^{3+} \rightarrow Eu^{3+} + Dy^{2+}$$

which was believed to delay the 520 nm emission because the reverse reaction is thermally activated.

3.4. Difficulties of the Existing Mechanisms. It is highly unlikely that the species Eu^{+}* and Dy^{4+} are generated under a UV or visible excitation. Furthermore, electronic band structure calculations carried out for $SrAl_2O_4:Eu^{2+}$ show that the Eu d-block bands lie just below the CB bottom.[17] This finding is consistent with preliminary XPS measurements, which locate the 4f-block levels of Eu^{2+} at approximately 3 eV above the VB top.[17] Thus, these observations definitely do not support the mechanism of Matsuzawa et al.

EPR measurements of $SrAl_2O_4:Eu^{2+},Dy^{3+}$ samples show that the concentration of Eu^{2+} decreases during the UV excitation and increases when the excitation is stopped until the extinction of phosphorescence.[23] This finding evidences that Eu^{2+} participates in the trapping process and, hence, does not support the idea of energy transfer to Eu^{2+} after the trapping, suggested by Aitasalo et al. and also by Beauger. In addition, the mechanism of Beauger for $SrAl_2O_4:Eu^{2+}$, Dy^{3+} is difficult to support because the lifetime of Dy^{2+} is certainly too short to explain the occurrence of phosphorescence lasting several hours.

4. New Phosphorescence Mechanism

As discussed above, the existing phosphorescence mechanisms are not consistent with a number of important experimental and theoretical observations. It is important to formulate a new mechanism for the phosphorescence of $SrAl_2O_4:Eu^{2+}$, with and without Dy^{3+} and/or B^{3+} codoping, that are consistent with the experimental and theoretical observations. Our mechanism, depicted in Figure 6, relies on the facts that the d orbitals of Eu^{2+} are located near the CB bottom of $SrAl_2O_4$, that the Eu^{2+} concentration decreases under UV excitation, and that the phosphor samples always have a small amount of Eu^{3+} ions because it is impossible to reduce all Eu^{3+} ions into Eu^{2+} ions under the synthetic conditions employed. Under UV irradiation, electrons are promoted from the occupied 4f levels of Eu^{2+} to the empty 5d levels and from the VB top to the unoccupied 4f levels

of residual Eu^{3+} (i.e., charge transfer). The electrons promoted to the 5d levels can be trapped at the V_O defects located in the vicinity of the photogenerated Eu^{3+} cations (see section 4.1 for further discussion), while the holes created in the VB can be trapped at the V_{Sr} or V_{Al} levels. Due to these trapping processes, Eu^{2+} is oxidized to Eu^{3+}, while residual Eu^{3+} is reduced to Eu^{2+}. The thermal energy at ambient temperature causes the detrapping of the trapped electrons directly to the 5d levels of Eu^{3+}, hence leading to the $4f^65d^1 \rightarrow 4f^7(^8S_{7/2})$ green phosphorescence. The 450 nm blue emission, observed only at low temperatures (below 150 K), is probably due to the charge transfer from the fundamental level of the $4f^7$ configuration of Eu^{2+} to the VB and is associated with a hole detrapping mechanism. In the following, we show that a number of experimental findings are consistent with our mechanism.

4.1. Origin of the Phosphorescence and Photoconductivity. To reconcile the position of the Eu^{2+} orbitals in the forbidden band with the variation of the Eu^{2+} concentration during UV excitation and phosphorescence, it is necessary to consider a trapping of the electrons promoted to the Eu^{2+} 5d levels under UV irradiation. Nevertheless, the existence of holes in the VB observed by photoconductivity has to be addressed first.

The band gap of $SrAl_2O_4$ is 6.5 eV,[27] so that no transition between the VB and CB can occur under UV irradiation. Beauger assigned the 450 nm blue emission to the de-excitation from a discrete level of unknown origin located in the middle of the forbidden gap to the valence band.[8] The levels associated with the cation or anion vacancies are generally close to the VB top or the CB bottom (as shown for $SrAl_2O_4$ by calculations[17]), so it is unlikely that they are responsible for the excitation energy of $\sim$3 eV.[29] As already mentioned, the $4f^7(^8S_{7/2})$ level of Eu^{2+} is located at 3 eV above the VB top. Thus, the 450 nm emission could be assigned to the transition from this level to the VB, after a charge transfer from O^{2-} to residual Eu^{3+} cations.

At this point, it is necessary to distinguish our assignment of the 450 nm emission from the one commonly assigned to the Eu^{3+} cations, for example in Y_2O_3:Eu^{3+}.[1] In the latter assignment, excitation takes place by a charge-transfer absorption from oxygen to europium, i.e.,

$$Eu^{3+}\,(4f^6) + O^{2-}\,(2p^6) \rightarrow Eu^{2+}{}^*\,(4f^7) + O^{-}\,(2p^5)$$

Then, concomitantly with a charge transfer from europium to oxygen, an electron of the Eu cation de-excites non-radiatively to form the excited state $4f^{6*}$ (e.g., $^5D_2$, $^5D_1$, $^5D_0$ states) of Eu^{3+}, which subsequently leads to the ground state $4f^6$ ($^7F_0$) of Eu^{3+} via a $4f \rightarrow 4f$ radiative transition. The $Eu^{2+}{}^*$ intermediate state thus created should have a very short lifetime because the host lattice provides a higher stability for Eu^{3+} than for Eu^{2+} (in the Y^{3+} site). However, this is not the case for $SrAl_2O_4$:Eu^{2+}, because Eu^{2+} ions are located at the Sr^{2+} sites.

Whereas $SrAl_2O_4$:Eu^{2+} is conductive after stopping the excitation, it is noted that the characterization of its mobile carriers as holes was determined only during the UV irradiation.[25] Thus, one might question if the holes are really trapped. The TL curves of $SrAl_2O_4$:Eu^{2+} measured between 75 and 475 K (with a heating rate of 5 or 30 K/min leading to slight changes in peak positions) present at least 10 peaks (at 105, 120, 135, 165, 190, 215, 245, 275, 305, and 345 K),[4,8,25] which indicates the presence of 10 or more traps in the host lattice with different depths. The spectral analysis of the glow curve indicates that the TL peak at 105 K is associated with the 450 and 520 nm emissions.[8] Since no energy transfer can occur from a 520 nm emission to a 450 nm emission, the activation of the 450 nm emission proves definitely that some holes are trapped.

The observation of a hole-type photoconductivity at room temperature in $SrAl_2O_4$:Eu^{2+} does not necessarily mean that the charge carriers consist solely of holes. Indeed, even if conductivity has contributions from holes and electrons, an overall hole-type conductivity is observed if the contribution of holes dominates over that of electrons. Thus, one might speculate if both holes and electrons contribute to the photoconductivity.

The measurement of the temperature dependence of the photoconductivity under UV excitation gives the total number of charge carriers (at least holes) released by the supply of thermal energy. To some extent, the sum of the charge carriers released when the temperature is continuously increased is related to the integral of a thermo-conductivity curve without UV excitation. For $SrAl_2O_4$:Eu^{2+},Dy^{3+}, the photoconductivity under irradiation increases from about 80 K up to 250 K, and then a plateau is reached until 300 K.[4] Thus, there occurs no detrapping phenomenon involving conductivity at 300 K. However, the TL measurements show a strong detrapping phenomenon at 300 K, leading to phosphorescence.[4] Therefore, it is necessary to suppose that detrapped electrons do not migrate in the CB, and that photoconductivity is due only to holes. This conclusion leads to the supposition that the electron traps are present in the vicinity of the photogenerated Eu^{3+} cations so that they can recombine without contributing to the electric conductivity.

In the present case, the consideration of the proximity of the electron trap around the activator (i.e., the photogenerated Eu^{3+} cation) is reasonable because there is no overlap between the occupied discrete orbitals of the electron trap and the 4f orbitals of the activator. This makes direct recombination impossible and hence electron detrapping thermally activated. Electron detrapping can occur from the oxygen vacancy levels either to the 5d orbitals of the photogenerated Eu^{3+} or to the CB (i.e., to strongly localized levels of the lattice resulting from the local deformation associated with defects). To find which of the two detrapping processes is appropriate, we consider the evolution of the TL curves of the alkaline-earth aluminates AAl_2O_4 series (A = Ca, Sr, Ba). The TL curves of $Ca_{0.98}Al_2O_4$:$Eu^{2+}{}_{0.02}$, $Sr_{0.98}Al_2O_4$:$Eu^{2+}{}_{0.02}$, and $Ba_{0.98}Al_2O_4$:$Eu^{2+}{}_{0.02}$ [17] presented in Figure 7 indicate that the three main peaks move toward a higher temperature (i.e., toward a greater trap depth) on going from Sr to Ba to Ca. Whereas the bottom of CB is expected to go up in energy in the order Ca (3d) < Sr (4d) < Ba (5d), the energies of the $4f^65d^1 \rightarrow 4f^7$ ($^8S_{7/2}$) emission of Eu^{2+} (and thus the position of the bottom of 5d orbitals of Eu^{2+}) increase in the order Sr (2.38 eV) < Ba (2.48 eV)

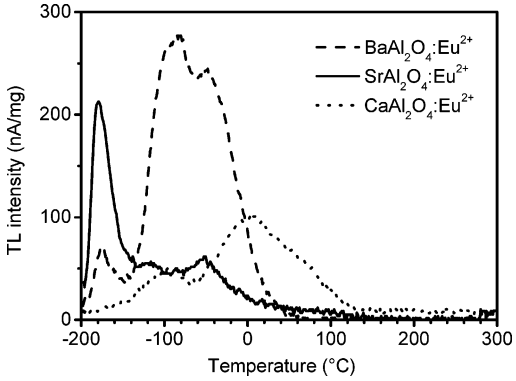

Figure 7. TL curves of $Ba_{0.98}Al_2O_4:Eu^{2+}_{0.02}$ (dashed line), $Sr_{0.98}Al_2O_4:Eu^{2+}_{0.02}$ (full line), and $Ca_{0.98}Al_2O_4:Eu^{2+}_{0.02}$ (dotted line), measured after 5 min of irradiation at 254 nm with a heating rate of 30 °C/min.

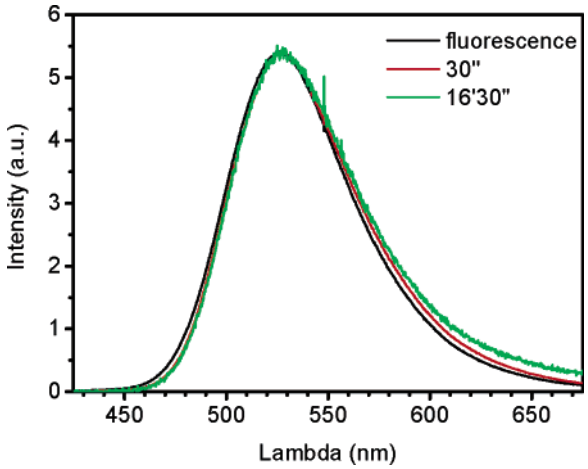

Figure 8. Evolution of the 520 nm luminescence peak (normalized) for $Sr_{0.98}Al_2O_4:Eu^{2+}_{0.02}$ in fluorescence (in black), after 0.5 min of phosphorescence (in red), and after 16.5 min of phosphorescence (in green), which was measured after 5 min of irradiation at 310 nm, using a Fluorolog-3 spectrofluorometer equipped with a CCD detector.

< Ca (2.82 eV), i.e., in the same order as do the TL peaks. This suggests that the electron detrapping occurs toward the 5d orbitals of Eu^{2+}. This proposition is consistent with TL experiments carried out for new phosphorescent compounds recently patented. Furthermore, the very intense fluorescence of $SrAl_2O_4:Eu^{2+}$ leads us to suppose that the photoionization rate of electrons from the 5d orbitals to the CB is weak.

Several observations confirm the proximity of the electron trap around the luminescent center. First, it explains the absence of EPR signal associated with electrons during trapping, because a strong spin−orbit coupling between the trapped electron and the Eu^{3+} ion widens the EPR peak, which then becomes undetectable. Second, it explains why the emission spectra of $SrAl_2O_4:Eu^{2+}$ in fluorescence and in phosphorescence are different (Figure 8): the environment of the Eu^{2+} causing the phosphorescence is different from that of the Eu^{2+} causing the fluorescence, due probably to the presence of the electron trap in its vicinity. This shift may reach 10 nm in $CaAl_2O_4:Eu^{2+}$ (440 nm against 430 nm).[34]

It is important to determine whether phosphorescence is also related to the hole trapping, in other words, whether any energy transfer occurs between the 450 and 520 nm emissions at ambient temperature. Indeed, the intensity decrease in the 450 nm emission between 150 and 270 K[8] can be due either to a thermal quenching or to a thermally activated energy transfer. The photoconductivity decay time of $SrAl_2O_4:Eu^{2+},Dy^{3+}$, which is due only to holes, is much longer than the 520 nm phosphorescence decay time at room temperature (i.e., several days vs several hours).[35] Thus, the phosphorescence cannot be caused by both electrons and holes, but is due solely to electrons. Consequently, at ambient temperature, the photoconductivity and the phosphorescence should originate from two different electronic phenomena, and the blue emission should be thermally quenched.

4.2. Nature of the Electron and Hole Traps. The codoping of $SrAl_2O_4:Eu^{2+}$ with Y^{3+} decreases the 450 nm emission intensity.[8] Interstitial oxygen atoms cannot be present since the synthesis atmosphere is reducing in nature. Thus, cation vacancies are expected to act as hole traps. Because the formation of aluminum vacancies is energetically unfavorable, the strontium vacancies should be the major hole traps.

The phosphorescence of $SrAl_2O_4:Eu^{2+}$ is enhanced with increasing the Sr^{2+} deficiency[25,36] and is reduced upon substituting Si^{4+} for Al^{3+}.[32] Due to the charge neutrality requirement, the number of oxygen vacancies should increase by increasing the Sr^{2+} deficiency and should decrease by the substitution of Si^{4+} for Al^{3+}. Therefore, the oxygen vacancy levels V_O (in the vicinity of Eu^{2+}) are the electron traps.

To estimate the positions of the V_{Sr}, V_{Al}, and V_O levels within the band gap (~6.5 eV) of $SrAl_2O_4$, it is necessary to know the orbital nature of not only these vacancy levels but also the VB top and the CB bottom. For simplicity, we suppose that each Al^{3+} is sp^3-hybridized, and so is each O^{2-}. Then, every sp^3 orbital of Al^{3+} is empty while every sp^3 orbital of O^{2-} is doubly occupied. The σ-bonding (σ_{Al-O}) and the σ^*-antibonding (σ^*_{Al-O}) levels of an Al−O bond are respectively formed by the in-phase and out-of-phase combinations of the sp^3 orbitals of the Al^{3+} and O^{2-} ions. Electronic band structure calculations based on density functional theory (DFT) [17] reveal that the top portion of the VB's are represented by the oxygen lone pair levels (i.e., the sp^3 orbitals of O^{2-}), the CB's are represented by the σ^*_{Al-O} levels, and the bottom portion of the CB's overlaps with the bands arising from the 4d orbitals of the Sr^{2+} ions.

An oxygen vacancy generates three-coordinate pyramidal AlO_3 units, in which one sp^3 orbital of the Al atom has lost an oxygen sp^3 orbital to make bonding/antibonding interaction with. Therefore, the V_O level corresponds to an empty sp^3 orbital of Al^{3+}, which should lie considerably below the CB bottom, because of the strength of the Al−O bond. Due to the proximity between the Sr and O atoms, the orbitals of the Sr adjacent to this O vacancy point toward this vacancy site.

The lone pair orbitals of the oxygen atoms surrounding the Sr^{2+} vacancy are not stabilized with respect to those of

(34) Hölsa, J.; Jungner, H.; Lastusaari, M.; Niittykoski, J. *J. Alloys Compd.* **2001**, *323*, 326.

(35) Yuan, H.; Jia, W.; Basun, S.; Lu, L.; Meltzer, R.; Yen, W. *J. Electrochem. Soc.* **2000**, *147*, 3154.

(36) Aitasalo, T.; Hölsa, J.; Lastusaari, M.; Legendziewicz, J.; Niittykoski, J. *Radiat. Eff. Defects Solids* **2003**, *158*, 89.

the oxygen atoms surrounding the Sr^{2+} cations. Consequently, the V_{Sr} level is essentially the nonstabilized oxygen lone pair level, which should lie slightly above the top of the valence bands.

The pocket of four O^{2-} ions surrounding an Al^{3+} vacancy would cause a significant destabilization due to the overlap repulsion between the sp^3 orbitals of the four O^{2-} ions and to Coulomb repulsion between the four O^{2-} ions. Thus, the V_{Al} levels should correspond to the oxygen lone pair levels lying significantly above the VB top and could act as a strong hole trap.

DFT electronic band structure calculations of $SrAl_2O_4$ with Sr and O vacancies show that the V_{Sr} is located at 0.15 eV above the VB top, and the V_O level is at 0.60 eV below the CB bottom.[17] These values are subject to errors but evidence that the electron trap level V_O is significantly deeper than the hole trap level V_{Sr}.

The thermal quenching of the 450 nm emission from 150 K prevents from detecting any deep hole traps by TL measurements. However, the conductivity is here associated only with hole traps, so their depths can be determined from thermo-conductivity measurements. The temperature dependence of the photoconductivity of $SrAl_2O_4$:Eu^{2+},Dy^{3+} measured by Matsuzawa et al. between 70 and 300 K[4] (described above) shows that the hole traps correspond to detrapping temperatures from 80 K up to 250 K. As the thermoluminescence of $SrAl_2O_4$:Eu^{2+},Dy^{3+} measured by Beauger[8] presents a main peak from 230 K up to 440 K (i.e., the temperatures for which the 450 nm emission is thermally quenched), it is confirmed that the electron traps V_O are overall deeper than the hole traps V_{Sr}.

4.3. Role of the Dy^{3+} and B^{3+} Codopants. The phosphorescence of $SrAl_2O_4$:Eu^{2+} is improved largely by codoping with Dy^{3+}.[4] Nevertheless, the oxidation or reduction of Dy^{3+} is unlikely to occur under excitation in the visible,[7] so the role of Dy^{3+} should be indirect. The variation of the TL curve upon the codoping suggests that the Dy^{3+} cation increases the number and the depth of the electron traps.[8] From the viewpoint of charge balance, however, the substitution of Ln^{+3} for Sr^{2+} (Ln = lanthanide) should disfavor the occurrence of O^{2-} vacancies. In addition, both Ln_{Sr}° and $V_O^{\circ\circ}$ defects induce electron deficiency in their environment, so they should repel each other and hence Dy^{3+} may not influence the trap depth of the oxygen vacancies. Thus, at this stage, it remains unclear how the codopants Dy^{3+} improve the phosphorescence in $SrAl_2O_4$:Eu.

As already mentioned, the electronic band structure calculations show that the strontium orbitals contribute to the oxygen vacancy level. It would be reasonable to suppose that the orbitals of Eu^{2+} (and Dy^{3+}) do so as well when the dopants (and codopants) are in its vicinity. An anion vacancy requires some electron density to gain stability. Thus, it is important to consider the ability of the surrounding cations to delocalize their electron density toward the vacancy. The ionization potential of a cation (e.g., $Sr^{2+} \rightarrow Sr^{3+} + e^-$) would be an appropriate parameter to gain insight into its ability to reorganize its electron cloud toward the anion vacancy. The lower the ionization potential of the cation, the greater is the ability of the cation to stabilize the oxygen vacancy, and the more strongly V_O is attracted to the cation. The ionization potentials of Eu^{2+}, Dy^{3+}, and Sr^{2+} are 25.0, 41.5, and 43.7 eV, respectively. This means that V_O defects are attracted to Eu^{2+} cations thereby becoming electron traps, and the presence of a Dy^{3+} cation (with a lower ionization potential than Sr^{2+}) near Eu^{2+} would reinforce the influence of Eu^{2+} on V_O. The higher number of anion vacancies in the vicinity of Eu^{2+} (i.e., that of electron traps) as well as the greater stabilization of V_O (i.e., the greater trap depth) lead to a better phosphorescence upon codoping with Dy^{3+}.

We probe the implication of the above discussion further by examining how the ionization potentials of other Ln^{3+} codopants influence the phosphorescence. This ionization potentials of Ln^{3+} cations increases in the order[37] Ce < Pr < Tb < Nd < Sm < Dy < Ho < Eu < Er < Tm < Yb < Gd < Lu < La < Y.

From this series, we exclude the Eu^{3+} ion because its intrinsic concentration at the thermodynamic equilibrium in the phosphor is very low. In addition, we discard the Sm^{3+} and Yb^{3+} ions due to the stabilization of their +2 species in the material,[7,38] and Ce^{3+}, Pr^{3+}, and Tb^{3+} ions due to the stability of their +4 oxidation state. Then, the ionization potentials of the remaining cations and those of the alkaline-earth cations Sr and Ca, show the order Nd < Dy < Ho < Er < Tm < Sr < Gd < Lu < La < Ca < Y.

This trend is opposite to that in the phosphorescence decay time of $SrAl_2O_4$:Eu^{2+},Ln^{3+} with respect to that of the un-co-doped $SrAl_2O_4$:Eu, which decreases in the order[8,39] Dy > Nd ≫ Ho > Er > un-codoped > Gd > Y.

The phosphorescence decay time of $CaAl_2O_4$:Eu^{2+},Ln^{3+} exhibits a similar trend,[39] i.e., Nd > Dy > Ho > Er > un-codoped.

As another support for our reasoning, we note that the ionization potential of Eu^{3+} is lower than that of Sr^{2+} (42.71 vs 43.71 eV). This explains why the phosphorescence properties are improved by preheating under air,[23] because the latter can lead to more oxygen vacancies around Eu^{2+}.

The improvement of phosphorescence upon codoping with B^{3+} could be due to an increase in the oxygen vacancy concentration (probably related to the appearance of three-coordinate BO_3 units). Nevertheless, these vacancies are not necessarily close enough to Eu^{2+} to act as electron traps. Another reason might be the creation of acceptor levels lying within the forbidden gap due to the ability of boron to adopt a triangular planar BO_3 configuration. The replacement of Al^{3+} by a sp^2-hybridized B^{3+} leads to an empty 2p orbital at the B^{3+} site, which should lie considerably below the CB bottom. This replacement also leads to an sp^3 orbital of the oxygen uncoordinated to B^{3+}, which should lie above the VB top. Such a hypothesis predicts extra peaks in TL, but they have not been observed at all.[40] Finally, we note that

(37) Emsley, J. *The elements*; Clarendon Press: Oxford, 1989.
(38) Aitasalo, T.; Deren, P.; Hölsa, J.; Jungner, H., Lastusaari, M.; Niittykoski, J.; Strek, W. *Radiat. Meas.* **2004,** *38*, 515.
(39) Zhang, T.; Su, Q. *J. Soc. Inform. Dis.* **2000**, *8*, 27.
(40) Niittykoski, J.; Aitasalo, T.; Hölsa, J.; Jungner, H.; Lastusaari, M.; Parkkinen, M.; Tukia, M. *J. Alloys Compd*. **2004**, *374*, 108.
(41) Sakai, R.; Katsumata, T.; Komuro, S.; Morikawa, T. *J. Lumin.* **1999**, *85*, 149.
(42) Jia, D.; Yen, W. *J. Lumin.* **2003**, *101*, 115.
(43) Jia, D.; Yen, W. *J. Electrochem. Soc.* **2003**, *150*, H61.

B^{3+} has a higher ionization potential than does Al^{3+} (259.8 eV vs 120.2 eV), and this would cause its migration toward Eu^{2+} (with very low ionization potential) and thus toward the electron traps V_O. The strong participation of the orbitals of B^{3+} in the formation of the discrete level associated with V_O causes then a slight change in the depth.[40]

5. Concluding Remarks

The existing mechanisms of luminescence proposed to explain the long lasting phosphorescence of $SrAl_2O_4:Eu^{2+},Dy^{3+}$ and related phosphors cannot accommodate a number of experimental and theoretical observations. On the basis of the fact that the d orbitals of Eu^{2+} are located near the CB bottom, Eu^{2+} concentration decreases under UV excitation, and trace amounts of Eu^{3+} are always present in these compounds, we formulated a new mechanism of phosphorescence in which Eu^{2+} ions are oxidized to Eu^{3+} under UV, the released electrons are trapped at oxygen vacancies in the vicinity of a photogenerated Eu^{3+}, and the phosphorescence arises from the recombination of the trapped electrons at the photogenerated Eu^{3+} sites with emission at 520 nm. Another emission of $SrAl_2O_4:Eu^{2+},Dy^{3+}$ at 450 nm, which occurs at low temperatures, arises from a charge transfer from oxygen to residual Eu^{3+} that takes place upon UV irradiation and is associated with a hole trapping at Sr^{2+} vacancies. Our study indicates that codoping with Dy^{3+} enhances the phosphorescence because it increases the number of electron traps in the vicinity of Eu^{2+} and their trap depth.

Acknowledgment. The research has been made possible by a grant (9504213.00) from Rhodia Electronics & Catalysis. The authors acknowledge Professor D. Gonbeau (LCTPCM, Pau), Doctor P. Bonville (CEA, Saclay), and Professor P. Iacconi (Université de Nice) for preliminary XPS, Mössbauer, and thermoluminescence measurements, respectively, on $SrAl_2O_4$:Eu during the course of research collaboration on our unpublished, patented phosphorescent materials. The work at NCSU was supported by the Office of Basic Energy Sciences, Division of Materials Sciences, U.S. Department of Energy, under Grant DE-FG02-86ER45259.

CM050763R

(44) Jia, D.; Wang, X.; Jia, W.; Yen, W. *J. Appl. Phys.* **2003**, *93*, 148.
(45) Jüstel, T.; Bechtel, H.; Mayr, W.; Wiechert, D. *J. Lumin.* **2003**, *104*, 137.
(46) Jia, D.; Wang, X.; van der Kolk, E.; Yen, W. *Opt. Commun.* **2002**, *204*, 247.
(47) Nakagawa, H.; Ebisu, K.; Zhang, M.; Kitaura, M. *J. Lumin.* **2003**, *102*−*103*, 590.
(48) Jia, D.; Wang, X.; Yen, W. *Chem. Phys. Lett.* **2002**, *363*, 241.
(49) Lin, Y.; Tang, Z.; Zhang, Z. *Mater. Lett.* **2001**, *51*, 14.
(50) Chang, C.; Mao, D.; Shen, J.; Feng, C. *J. Alloys Compd.* **2003**, *348*, 224.
(51) Kodama, N.; Takahashi, T.; Yamaga, M.; Tanii, Y.; Qiu, J.; Hirao, K. *Appl. Phys. Lett.* **1999**, *75*, 1715.
(52) Zhang, J.; Zhang, Z.; Wang, T.; Hao, W. *Mater. Lett.* **2003**, *57*, 4315.
(53) Lin, Y.; Tang, Z.; Zhang, Z.; Nan, C. *J. Alloys Compd.* **2003**, *348*, 76.
(54) Lin, Y.; Nan, C.; Zhou, X.; Wu, J.; Wang, H.; Chen, D.; Xu, S. *Mater. Chem. Phys.* **2003**, *82*, 860.
(55) Jiang, L.; Chang, C.; Mao, D. *J. Alloys Compd.* **2003**, *360*, 193.
(56) Jiang, L.; Chang, C.; Mao, D.; Zhang, B. *Mater. Lett.* **2004**, *58*, 1825.
(57) Wang, X.; Jia, D.; Yen, W. *J. Lumin.* **2003**, *102*, 34.
(58) Lei, B.; Liu, Y.; Ye, Z.; Shi, C. *J. Lumin.* **2004**, *109*, 215.
(59) Lei, B.; Liu, Y.; Liu, J.; Ye, Z.; Shi, C. *J. Solid State Chem.* **2004**, *177*, 1333.
(60) Kodama, N.; Sasaki, N.; Yamaga, M.; Masui, Y. *J. Lumin.* **2001**, *94*−*95*, 19.
(61) Yamaga, M.; Tanii, Y.; Kodama, N.; Takahashi, T.; Honda, M. *Phys. Rev. B* **2002**, *65*, 235108.
(62) Wang, Y.; Wang, Z.; Zhang, P.; Hong, Z.; Fan, X.; Qian, G. *Mater. Lett.* **2004**, *58*, 3308.
(63) Uheda, K.; Maruyama, T.; Takizawa, H.; Endo, T. *J. Alloys Compd.* **1997**, *262*−*263*, 60.
(64) Fu, J. *Electrochem. Solid State Lett.* **2000**, *3*, 350.
(65) Fu, J. *J. Am. Ceram. Soc.* **2002**, *85*, 255.
(66) Lin, Y.; Nan, C.; Cai, N.; Zhou, X.; Wang, H.; Chen, D. *J. Alloys Compd.* **2003**, *361*, 92.
(67) Wang, J.; Wang, S.; Su, Q. *J. Solid State Chem.* **2004**, *177*, 895.
(68) Iwasaki, M.; Nam Kim, D.; Tanaka, K.; Murata, T.; Morinaga, K. *Sci. Technol. Adv. Mater.* **2003**, *4*, 137.
(69) Wang, X.; Zhang, Z.; Tang, Z.; Lin, Y. *Mater. Chem. Phys.* **2003**, *80*, 1.
(70) Lei, B.; Liu, Y.; Tang, G.; Ye, Z.; Shi, C. *Mater. Chem. Phys.* **2004**, *87*, 227.
(71) Lei, B.; Liu, Y.; Tang, G.; Ye, Z.; Shi, C. *Chem. J. Chin. Univ.* **2003**, *24*, 782.
(72) Jia, D.; Jia, W.; Evans, D.; Dennis, W.; Liu, H.; Zhu, J.; Yen, W. *J. Appl. Phys.* **2000**, *88*, 3402.
(73) Jia, D.; Zhu, J.; Wu, B. *J. Electrochem. Soc.* **2000**, *147*, 386.
(74) Guo, C.; Zhang, C.; Lü, Y.; Tang, Q.; Su, Q. *Phys. Status Solidi A* **2004**, *201*, 1588.